Driving to the steady ground-state superposition assisted by spontaneous emission

Ming-Feng Chen, Li-Tuo Shen, Rong-Xin Chen, and Zhen-Biao Yang*
Department of Physics, Fuzhou University, Fuzhou 350116, P.R. China
(Received 17 June 2015; published 4 September 2015)

We propose a scheme for preparing a coherent ground-state superposition for an atom through external drivings assisted by spontaneous emission. In the scheme, the dynamics induced by the competition between the spontaneous emission and the external drives contributes to the superposition of the ground states. Compared with schemes based on the stimulated Raman adiabatic passage, such a scheme is more easily implemented because the preparation of special initial states is no longer needed, which simplifies the operation process. Moreover, since spontaneous emission is involved to act as a positive factor, a higher fidelity superposition state is achieved.

DOI: 10.1103/PhysRevA.92.033403 PACS number(s): 32.80.Qk, 42.50.−p

I. INTRODUCTION

A quantum computer overtakes its classical counterpart due to its fascinating feature, namely, the quantum superposition principle [1,2]. A lot of works devoted to the realization of superposition of multiple states have been published [3–13]. Most of these works are based on the stimulated Raman adiabatic passage (STIRAP) [3–10]. Note that in the STIRAP, the fidelity of the prepared superposition state is dependent on the specifically tailored pulse sequences of the laser fields. Besides, an initial state should be specified to determine what kind of laser fields should be used.

We should also notice that decoherence is unavoidable in a real experiment. It can decrease the coherence in a quantum system, ruining the reliability and practicality of quantum information. In recent years, the study of dissipation-induced state preparation has attracted many researchers' attention [14–18], showing that decoherence, if specifically tailored, could act as an effective factor assisting to drive the system to a more stable as well as a higher fidelity target quantum state. The effectiveness of decoherence has also been verified in entangled state preparation protocols because it exhibits good character in improving the fidelity of the target state as compared to those based on unitary dynamics [15,16].

In this paper, we present a scheme to prepare a single-atom ground-state superposition by the combination of coherent drivings and atomic spontaneous emission. The dynamics drives the atom with an arbitrary initial state to a specific superposition state formed by its ground states, optimally modulated by tuning the amplitude ratio between the laser fields. The validity of the analytical dynamics is verified by the numerical simulation, showing that the fidelity is remarkably improved due to the fact that the spontaneous emission is effectively employed. We will detail this by making a comparison with a previous scheme through STIRAP [6]. The scheme we propose here is also different from the theoretical work in [19,20] as well as the experimental work in [21] for the preparation of a specific qubit state, because those studies [19–21] are based on the assistance of the cavity field photon decay.

The paper is organized as follows. In Sec. II, the theoretical method to obtain the ground-state superposition is given. In Sec. III, detailed numerical simulation is discussed to approve the analytical dynamics. In Sec. IV, the generalization to the preparation of a n-ground-state superposition is made. The summary is given in Sec. V.

II. ANALYTICAL DISCUSSION

We first consider a three-level atom that possesses two ground states $|g_1\rangle$ and $|g_2\rangle$ and one excited state $|r\rangle$, as shown in Fig. 1. Such an atomic structure is common for preparing entangled states and implementing logic gates in experiment. Two laser fields are applied to drive the atomic transitions $|g_1\rangle \leftrightarrow |r\rangle$ and $|g_2\rangle \leftrightarrow |r\rangle$. The Rabi frequencies of these two laser fields are Ω_1 and Ω_2. Moreover, these two laser fields are assumed to be both detuned from the atomic transitions with the same detuning Δ. The Hamiltonian of the system in the interaction picture can be written as

$$H = (\Omega_1|g_1\rangle\langle r| + \Omega_2|g_2\rangle\langle r| + \text{H.c.}) + \Delta|r\rangle\langle r|. \quad (1)$$

The eigenvalues and eigenstates of the Hamiltonian H are listed in Table I. N_1, N_2, and N_3 are the corresponding normalization constants of the eigenstates $|\psi_1\rangle$, $|\psi_2\rangle$, and $|\psi_3\rangle$, respectively. The eigenstate with null eigenvalue is formed by the superposition of the two ground states. Such a state is of importance since it can be the initial state for protocols of entangled state preparation [22,23]. Here we would like to prepare this kind of superposition state by utilizing the dynamics induced by the coherent drivings as well as the decaying of the excited state (with κ_1 and κ_2 denoting the decay rates for its spontaneous emission to the two ground states). The time evolution of the density matrix of the system is described by the Markovian master equation

$$\dot{\rho} = -i[H,\rho] + \sum_{j=1}^{2} \frac{\kappa_j}{2}(2S_j\rho S_j^\dagger - S_j^\dagger S_j\rho - \rho S_j^\dagger S_j), \quad (2)$$

where $S_j = |g_j\rangle\langle r|$. One intuitive way to solve the problem is to use the eigenstates of the Hamiltonian and rewrite the motion of the density matrix in the dressed state picture based on the eigenstate basis. Under the eigenstate basis space $\{|\psi_1\rangle$,

*zbyang@fzu.edu.cn

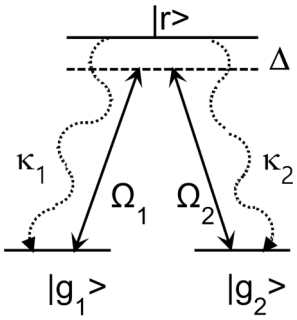

FIG. 1. Level configuration of the atom. Two laser fields are applied to drive the atomic transitions $|g_1\rangle \leftrightarrow |r\rangle$ and $|g_2\rangle \leftrightarrow |r\rangle$, with the corresponding Rabi frequencies being Ω_1 and Ω_2, respectively. κ_1 and κ_2 denote the rates for the excited state $|r\rangle$ decaying to the ground state $|g_1\rangle$ and $|g_2\rangle$, respectively.

$|\psi_2\rangle, |\psi_3\rangle\}$, we get new forms of S_1 and S_2,

$$S_1 = \begin{pmatrix} 0 & \frac{\lambda_2\Omega_2}{N_1N_2} & \frac{\lambda_3\Omega_2}{N_1N_3} \\ 0 & \frac{\lambda_2\Omega_1}{N_2^2} & \frac{\lambda_3\Omega_1}{N_2N_3} \\ 0 & \frac{\lambda_2\Omega_1}{N_2N_3} & \frac{\lambda_2\Omega_1}{N_3^2} \end{pmatrix},$$
$$S_2 = \begin{pmatrix} 0 & -\frac{\lambda_2\Omega_1}{N_1N_2} & -\frac{\lambda_3\Omega_1}{N_1N_3} \\ 0 & \frac{\lambda_2\Omega_2}{N_2^2} & \frac{\lambda_3\Omega_2}{N_2N_3} \\ 0 & \frac{\lambda_2\Omega_2}{N_2N_3} & \frac{\lambda_2\Omega_2}{N_3^2} \end{pmatrix}, \quad (3)$$

and thus Eq. (2) can be restructured. Notice that the value of the time differentiation of all the elements in the density matrix should come to zero when the system evolves to a steady state. We would like to discuss their influences on the steady ground-state superposition separately. First, we consider S_1 with decay rate κ_1, the detailed derivation process is presented in the Appendix. From the Appendix, we find that when the system evolves to a steady state under two coherent drivings and one decay channel, the system population finally transfers to $|\psi_1\rangle$. This is because the dark state $|\psi_1\rangle$ is the only eigenstate which does not contain the state component of the excited state $|r\rangle$, and its decaying finally dominates the evolution dynamics as the time increases when the coherent drivings are weak enough. Besides, it shows that an arbitrary initial state, not only a pure state but also a mixed state, is applicable for the generation of the state $|\psi_1\rangle$. It should be noticed that other methods like the STIRAP do not possess such an advantage. Dealing with S_2 with the decay rate κ_2, we will come to the same consequence. This means that these two decay processes are independent contribution sources for preparing the target state $|\psi_1\rangle$.

TABLE I. Eigenvalues and eigenstates for the Hamiltonian H.

Eigenvalue	Eigenstate
$\lambda_1 = 0$	$\|\psi_1\rangle = N_1(\Omega_2\|g_1\rangle - \Omega_1\|g_2\rangle)$
$\lambda_2 = \frac{\Delta-\sqrt{\Delta^2+4\Omega_1^2+4\Omega_2^2}}{2}$	$\|\psi_2\rangle = N_2(\Omega_1\|g_1\rangle + \Omega_2\|g_2\rangle + \lambda_2\|r\rangle)$
$\lambda_3 = \frac{\Delta+\sqrt{\Delta^2+4\Omega_1^2+4\Omega_2^2}}{2}$	$\|\psi_3\rangle = N_3(\Omega_1\|g_1\rangle + \Omega_2\|g_2\rangle + \lambda_3\|r\rangle)$

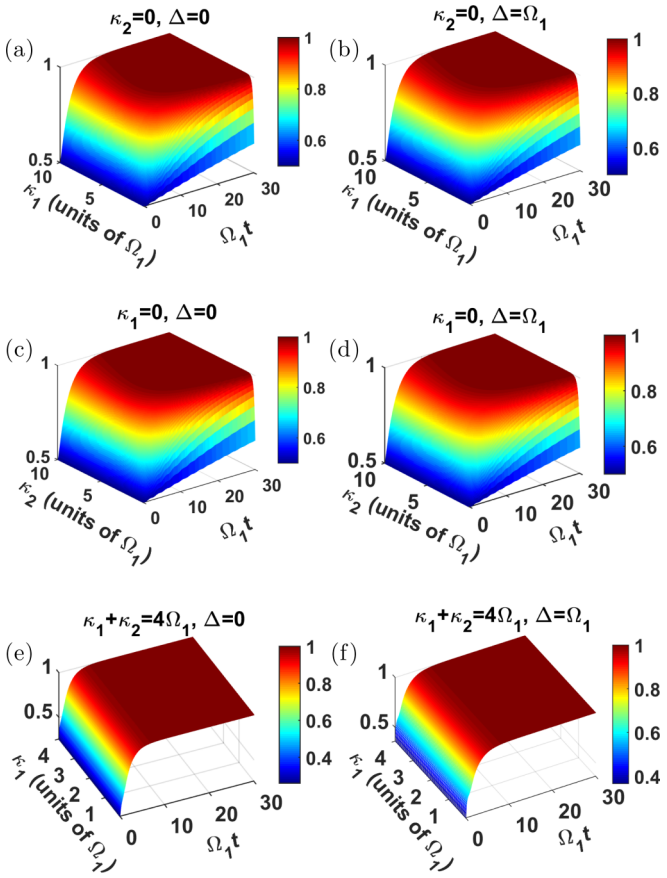

FIG. 2. (Color online) Population of the steady state $|\psi_s\rangle = \frac{1}{\sqrt{2}}(|g_1\rangle - |g_2\rangle)$ versus dimensionless parameter $\Omega_1 t$ and variable combination of κ_1 and κ_2 originating from a pure state $|g_1\rangle$ [(a),(b)] and from a mixed state $\frac{1}{2}(|g_1\rangle\langle g_1| + |g_2\rangle\langle g_2|)$ [(c),(d)], and averaging from 100 groups of initial random pure states [(e),(f)]. $\Omega_1 = \Omega_2 = 1$ unit, $\Delta = 0$ in the left-side graphs and $\Delta = \Omega_1$ in the right-side graphs.

III. NUMERICAL SIMULATION

Numerical simulations are presented here to show the validity of our proposal. In Fig. 2, we simulate the population of the steady state $|\psi_s\rangle = \frac{1}{\sqrt{2}}(|g_1\rangle - |g_2\rangle)$ as a function of dimensionless parameter $\Omega_1 t$ during the irreversible dynamical evolution, under the conditions of zero Δ and nonzero Δ, respectively, by presetting the kinds of initial states. For all the graphs in Fig. 2, the Rabi frequencies of the two laser fields Ω_1 and Ω_2 are set to be the same as 1 unit and the six graphs indicate six groups of parameter combinations. In Figs. 2(a), 2(c), and 2(e), we assume that both the two ground states are resonantly coupled to the excited state $|r\rangle$ ($\Delta = 0$); while in Figs. 2(b), 2(d), and 2(f), we assume that there is a detuning for the two laser fields driving the transitions $|g_1\rangle \leftrightarrow |r\rangle$ and $|g_2\rangle \leftrightarrow |r\rangle$ ($\Delta = \Omega_1$). As mentioned before, not only a pure state but also a mixed state can be applied as the initial state for the preparation of the steady state. The comparison between Figs. 2(a) [2(b)] and 2(c) [(2(d)] indeed shows that our scheme does not require the special initial state. Both the pure state $|g_1\rangle$ and the mixed state $\frac{1}{2}(|g_1\rangle\langle g_1| + |g_2\rangle\langle g_2|)$ can finally evolve to the steady state

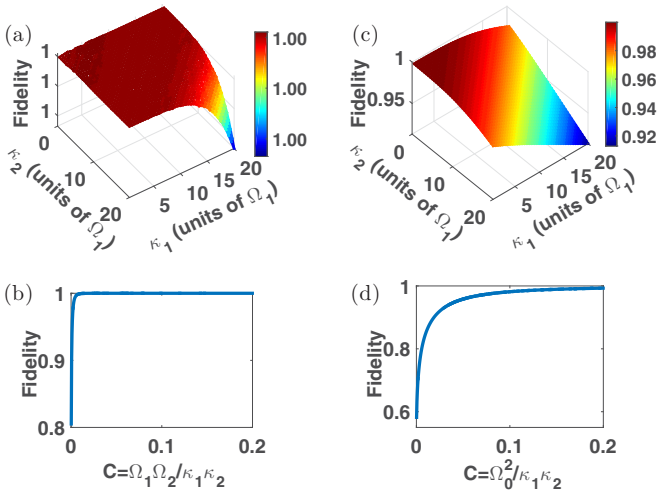

FIG. 3. (Color online) Comparison between our method [(a),(b)] and the STIRAP method [(c),(d)] to prepare the steady state $|\psi_s\rangle = \frac{1}{\sqrt{2}}(|g_1\rangle - |g_2\rangle)$ from a initial state $|g_1\rangle$. The dimensionless parameter $\Omega_1 t$ ranges from 0 to 100 for our method, while $\Omega_0 t$ ranges from 0 to 130 for the STIRAP method. $\Omega_0 = \Omega_1 = \Omega_2 = 1$ unit and $\Delta = 0$ are set.

$|\psi_s\rangle$. More generally, we use a random state generator to produce 100 groups of random initial pure states and average their results in Figs. 2(e) and 2(f). Besides, we find from Fig. 2 that the two decay channels are independent and have the same contribution on the preparation of the steady state. Therefore, they join together to promote the state preparation process. The detuning Δ would affect the evolution time, which can be concluded by comparing the left-side and right-side graphs in Fig. 2: the larger the detuning is, the longer the evolution time it takes. There exists an optimized value for the spontaneous decay rate, but the evolution rate is not proportional to the decay rate. Once the excitation is unstable and the decay rate is much stronger than the amplitude of the laser fields, it would cost more time for the system to decay to the target steady state.

To illustrate the advantage of our scheme, numerical results are shown below to compare our method with the one through the STIRAP for the preparation of the steady superposition $|\psi_s\rangle$ from a initial state $|g_1\rangle$. For the STIRAP method, we use two laser fields Ω_p and Ω_s referred in Ref. [6] to drive the transitions $|g_1\rangle \leftrightarrow |r\rangle$ and $|g_2\rangle \leftrightarrow |r\rangle$ [24], respectively. And we assume the condition of $\Delta = 0$ for both methods. Notice here that for the STIRAP method the pulse Ω_s comes first and is followed after a certain time delay by the other pulse Ω_p, and then the two pulses vanish simultaneously. While for our method, these two pulses remain the same all the time, and we assume them to be the same as 1 unit for simplicity. The time scales chosen for each method fulfill the required condition, which is the steady state condition for our method and the adiabatic condition for the STIRAP method. The dimensionless parameter $\Omega_1 t$ for our scheme is set to range from 0 to 100, and the $\Omega_0 t$ for the STIRAP is from 0 to 130. The fidelity [defined as $\langle\psi_s|\rho|\psi_s\rangle$, with ρ solved by the master equation in Eq. (2)] of the target state falls to 91.29% in Fig. 3(c) for STIRAP method, while that is close to 1 in Fig. 3(a) for our scheme (for both schemes, $\kappa_1 = \kappa_2 = 20\Omega_1$ is set). We define a quasi-cooperativity parameter $C = \Omega_1\Omega_2/\kappa_1\kappa_2$ for our method ($C = \Omega_0^2/\kappa_1\kappa_2$ for the STIRAP method). The relations between the cooperativity C and the fidelity are shown in Figs. 3(b) and 3(d). It shows that our method is more robust to the atomic spontaneous decay. As mentioned before, the fidelity can be improved by prolonging the evolution time if the decay rates are too large for our scheme. So the fidelity in Fig. 3(b) can be further improved by extending the evolution time.

IV. PREPARATION OF n-GROUND-STATE SUPERPOSITION

We can generalize the above method to the preparation of a single atom n-ground-state superposition. To tackle such a task, we need a more complex level configuration that involves $n-1$ auxiliary excited states as shown in Fig. 4. Such a level structure has been commonly employed in recent experiments (see Ref. [25] as an example).

The Rabi frequencies of the laser fields driving the ground state $|g_n\rangle$ are set to be Ω_n. All the laser fields are assumed to be detuned from the atomic transitions with the same detuning Δ. Under this situation, we obtain a dark state

$$|D_n\rangle = N_n \sum_{j=1}^{n} (-1)^{n-j} \frac{\Omega_n}{\Omega_j} |g_j\rangle, \tag{4}$$

where N_n is the normalization constant. By tuning the Rabi frequencies of the laser fields, we can get an arbitrary superposition state of the n ground states when the system is driven to be steady.

We should notice that the two laser fields applied on the same ground state $|g_n\rangle$ with unequal Rabi frequencies would lead to the deviation of the dark state $|D_n\rangle$. Nonetheless, our further numerical results show that the state $|D_n\rangle$ with a relative high fidelity can still be reached when the Rabi frequencies of these two laser fields are slightly different. For simplicity, we set the laser fields applied on the same ground state to be the same for the following numerical simulation. In Fig. 5, we use four groups of laser fields with preset Rabi frequencies (Ω_n) for preparing the superposition state $|D_n\rangle$ involving 2, 3, . . . , 12 ground states originating from a pure state $|g_1\rangle$. Each evolution line in the graphs corresponds to a different amount of laser fields applied to the system, which are picked out from the applied field group

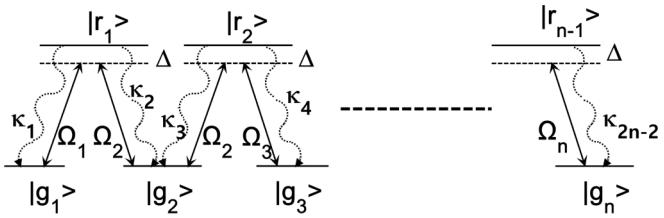

FIG. 4. Configuration for preparing an n-ground-state superposition. All the laser fields are detuned to the transition $|g_n\rangle \leftrightarrow |r_{n-1}\rangle$ and $|g_n\rangle \leftrightarrow |r_n\rangle$ with the same detuning Δ. The Rabi frequencies of the fields applied to the same ground state $|g_n\rangle$ are set to be the same as Ω_n. The excited state $|r_{n-1}\rangle$ is assumed to decay to the ground states $|g_n\rangle$ and $|g_{n+1}\rangle$ with decay rates κ_{2n-1} and κ_{2n}, respectively.

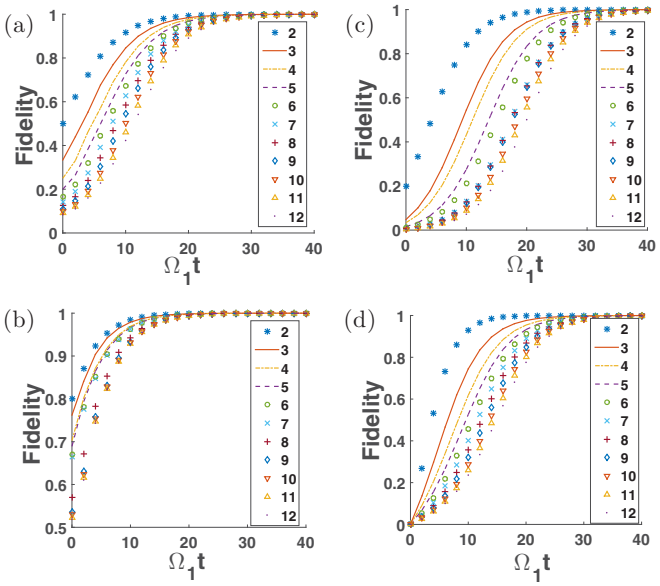

FIG. 5. (Color online) Population of the superposition state $|D_n\rangle$ involving $2, 3, \ldots, 12$ ground states originating from a pure state $|g_1\rangle$. The number in the legend represents the number of the ground states involved in the steady superposition state. Each graph corresponds to a set of laser fields of specific Rabi frequencies (Ω_n) with (a) {1, 1, 1, 1, 1, 1, 1, 1, 1, 1, 1} units; (b) {1, 2, 4, 3, 6, 5, 9, 2, 3, 7, 6, 8} units; (c) $\{1, \frac{1}{2}, \frac{1}{4}, \frac{1}{3}, \frac{1}{6}, \frac{1}{5}, \frac{1}{9}, \frac{1}{2}, \frac{1}{3}, \frac{1}{7}, \frac{1}{6}, \frac{1}{8}\} \times 13.1594$ units; (d) {100, 1, 1, 1, 1, 1, 1, 1, 1, 1, 1} units. $\Delta = 0$ is set. Notice that in (c) and (d) the axis $\Omega_1 t$ are respectively reduced 13.1594 and 100 times.

sequence in sequence. In this figure, we consider that each excited state $|r_n\rangle$ will decay to the related ground states $|g_n\rangle$ and $|g_{n+1}\rangle$ with the same decay rate (set to be 0.5 unit), and the detunings are set to be zero for simplicity. The numerical results show that the time required to reach the steady state slightly increases with increasing dimension of the superposition state.

V. SUMMARY

We have proposed a scheme to prepare the superposition of the ground states for a single atom, by the use of external fields assisted by spontaneous emission from the excited states. The scheme does not require the preparation of the specific initial states, relaxing the requirement for experimental implementation. As the spontaneous decay of the excited states is effectively employed in the process, the target state with a higher fidelity is achieved, as compared to the protocols through the unitary dynamics based on, for example, the STIRAP. Such a scheme may find many applications in quantum-information storage and processing.

ACKNOWLEDGMENTS

This work is supported by the Major State Basic Research Development Program of China under Grant No. 2012CB921601, the National Natural Science Foundation of China under Grants No. 11374054, No. 11305037, and No. 11405031, the Natural Science Foundation of Fujian Province under Grant No. 2014J05005, and funds from Fuzhou University.

APPENDIX

$$\dot{\rho_{11}} = \frac{\kappa_1}{2}\left\{2\left[\frac{\lambda_2\Omega_2}{N_1N_2}\left(\frac{\lambda_2\Omega_2}{N_1N_2}\rho_{22} + \frac{\lambda_3\Omega_2}{N_1N_3}\rho_{32}\right) + \frac{\lambda_3\Omega_2}{N_1N_3}\left(\frac{\lambda_2\Omega_2}{N_1N_2}\rho_{23} + \frac{\lambda_3\Omega_2}{N_1N_3}\rho_{33}\right)\right]\right\}, \tag{A1}$$

$$\begin{aligned}\dot{\rho_{12}} = & -i\lambda_2\rho_{12} + \left(\frac{\lambda_2\Omega_2}{N_1N_2}\rho_{22} + \frac{\lambda_3\Omega_2}{N_1N_3}\rho_{32}\right)\frac{\lambda_2\Omega_1}{N_2^2} + \left(\frac{\lambda_2\Omega_2}{N_1N_2}\rho_{23} + \frac{\lambda_3\Omega_2}{N_1N_3}\rho_{33}\right)\frac{\lambda_3\Omega_1}{N_2N_3} \\ & - \left[\left(\frac{\lambda_2\Omega_2}{N_1N_2}\right)^2 + \left(\frac{\lambda_2\Omega_1}{N_2^2}\right)^2 + \left(\frac{\lambda_2\Omega_1}{N_2N_3}\right)^2\right]\rho_{12} - \left(\frac{\lambda_2\lambda_3\Omega_2^2}{N_1^2N_2N_3} + \frac{\lambda_2\lambda_3\Omega_2^2}{N_2^3N_3} + \frac{\lambda_2\lambda_3\Omega_1^2}{N_2N_3^3}\right)\rho_{13},\end{aligned} \tag{A2}$$

$$\begin{aligned}\dot{\rho_{13}} = & -i\lambda_3\rho_{13} + \left(\frac{\lambda_2\Omega_2}{N_1N_2}\rho_{22} + \frac{\lambda_3\Omega_2}{N_1N_3}\rho_{32}\right)\frac{\lambda_2\Omega_1}{N_2N_3} + \left(\frac{\lambda_2\Omega_2}{N_1N_2}\rho_{23} + \frac{\lambda_3\Omega_2}{N_1N_3}\rho_{33}\right)\frac{\lambda_3\Omega_1}{N_3^2} \\ & - \left[\left(\frac{\lambda_3\Omega_2}{N_1N_3}\right)^2 + \left(\frac{\lambda_3\Omega_1}{N_2N_3}\right)^2 + \left(\frac{\lambda_3\Omega_1}{N_3^2}\right)^2\right]\rho_{13} - \left(\frac{\lambda_2\lambda_3\Omega_2^2}{N_1^2N_2N_3} + \frac{\lambda_2\lambda_3\Omega_2^2}{N_2^3N_3} + \frac{\lambda_2\lambda_3\Omega_1^2}{N_2N_3^3}\right)\rho_{12},\end{aligned} \tag{A3}$$

$$\begin{aligned}\dot{\rho_{22}} = & 2\left[\left(\frac{\lambda_2\Omega_1}{N_2^2}\rho_{22} + \frac{\lambda_3\Omega_1}{N_2N_3}\rho_{32}\right)\frac{\lambda_2\Omega_1}{N_2^2} + \left(\frac{\lambda_2\Omega_1}{N_2^2}\rho_{23} + \frac{\lambda_3\Omega_1}{N_2N_3}\rho_{33}\right)\frac{\lambda_3\Omega_1}{N_2N_3}\right] \\ & - 2\left[\left(\frac{\lambda_2\Omega_2}{N_1N_2}\right)^2 + \left(\frac{\lambda_2\Omega_1}{N_2^2}\right)^2 + \left(\frac{\lambda_2\Omega_1}{N_2N_3^3}\right)^2\right]\rho_{22} - 2\left(\frac{\lambda_2\lambda_3\Omega_2^2}{N_1^2N_2N_3} + \frac{\lambda_2\lambda_3\Omega_1^2}{N_2^3N_3} + \frac{\lambda_2\lambda_3\Omega_1^2}{N_2N_3^3}\right)\rho_{33},\end{aligned} \tag{A4}$$

$$\begin{aligned}\dot{\rho_{33}} = & 2\left[\left(\frac{\lambda_2\Omega_1}{N_2N_3}\rho_{22} + \frac{\lambda_3\Omega_1}{N_3^2}\rho_{32}\right)\frac{\lambda_2\Omega_1}{N_2N_3} + \left(\frac{\lambda_2\Omega_1}{N_2N_3}\rho_{23} + \frac{\lambda_3\Omega_1}{N_3^2}\rho_{33}\right)\frac{\lambda_3\Omega_1}{N_3^2}\right] \\ & - 2\left(\frac{\lambda_2\lambda_3\Omega_2^2}{N_1^2N_2N_3} + \frac{\lambda_2\lambda_3\Omega_1^2}{N_2^3N_3} + \frac{\lambda_2\lambda_3\Omega_1^2}{N_2N_3^3}\right)\rho_{22} - 2\left[\left(\frac{\lambda_3\Omega_2}{N_1N_3}\right)^2 + \left(\frac{\lambda_3\Omega_1}{N_2N_3}\right)^2 + \left(\frac{\lambda_3\Omega_1}{N_3^2}\right)^2\right]\rho_{33},\end{aligned} \tag{A5}$$

$$\dot{\rho_{23}} = -i(\lambda_2-\lambda_3)\rho_{23} + \frac{\kappa_1}{2}\left(2\left[\frac{\lambda_2\Omega_1}{N_2N_3}\left(\frac{\lambda_2\Omega_1}{N_2^2}\rho_{22}+\frac{\lambda_3\Omega_1}{N_2N_3}\rho_{32}\right)+\frac{\lambda_3\Omega_1}{N_3^2}\left(\frac{\lambda_2\Omega_1}{N_2^2}\rho_{23}+\frac{\lambda_3\Omega_1}{N_2N_3}\rho_{33}\right)\right]\right.$$
$$-\left\{\left[\left(\frac{\lambda_2\Omega_2}{N_1N_2}\right)^2+\left(\frac{\lambda_2\Omega_1}{N_2^2}\right)^2+\left(\frac{\lambda_2\Omega_1}{N_2N_3}\right)^2\right]\rho_{23}+\left[\frac{\lambda_2\lambda_3\Omega_2^2}{N_1^2N_2N_3}+\frac{\lambda_2\lambda_3\Omega_1^2}{N_2^3N_3}+\frac{\lambda_2\lambda_3\Omega_1^2}{N_2N_3^3}\right]\rho_{33}\right\}$$
$$\left.-\left\{\left[\frac{\lambda_2\lambda_3\Omega_2^2}{N_1^2N_2N_3}+\frac{\lambda_2\lambda_3\Omega_1^2}{N_2^3N_3}+\frac{\lambda_2\lambda_3\Omega_1^2}{N_2N_3^3}\right]\rho_{22}+\left[\left(\frac{\lambda_3\Omega_2}{N_1N_3}\right)^2+\left(\frac{\lambda_3\Omega_1}{N_2N_3}\right)^2+\left(\frac{\lambda_3\Omega_1}{N_3^2}\right)^2\right]\rho_{23}\right\}\right). \tag{A6}$$

The time differentiation of all the elements in the density matrix should be equal to zero when the system is steady. Because ρ_{23} is the complex conjugate of ρ_{32}, from Eq. (A1) we get a relation among ρ_{22}, ρ_{33}, and the real part of ρ_{23},

$$\mathrm{Re}\{\rho_{23}\} = -\frac{N_1^2N_2N_3}{2\lambda_2\lambda_3\Omega_2^2}\left[\left(\frac{\lambda_2\Omega_2}{N_1N_2}\right)^2\rho_{22}+\left(\frac{\lambda_3\Omega_2}{N_1N_3}\right)^2\rho_{33}\right]. \tag{A7}$$

Equations (A4) and (A5) also can be simplified as follows:

$$\frac{2\lambda_2\lambda_3\Omega_1^2}{N_2^3N_3}\mathrm{Re}\{\rho_{23}\}-\left[\left(\frac{\lambda_2\Omega_2}{N_1N_2}\right)^2+\left(\frac{\lambda_2\Omega_1}{N_2N_3^3}\right)^2\right]\rho_{22}-\left[\frac{\lambda_2\lambda_3\Omega_2^2}{N_1^2N_2N_3}+\frac{\lambda_2\lambda_3\Omega_1^2}{N_2^3N_3}+\frac{\lambda_2\lambda_3\Omega_1^2}{N_2N_3^3}-\left(\frac{\lambda_3\Omega_1}{N_2N_3}\right)^2\right]\rho_{33}=0, \tag{A8}$$

$$\frac{2\lambda_2\lambda_3\Omega_1^2}{N_2N_3^3}\mathrm{Re}\{\rho_{23}\}-\left[\frac{\lambda_2\lambda_3\Omega_2^2}{N_1^2N_2N_3}+\frac{\lambda_2\lambda_3\Omega_1^2}{N_2^3N_3}+\frac{\lambda_2\lambda_3\Omega_1^2}{N_2N_3^3}-\left(\frac{\lambda_2\Omega_1}{N_2N_3}\right)^2\right]\rho_{22}-\left[\left(\frac{\lambda_3\Omega_2}{N_1N_3}\right)^2+\left(\frac{\lambda_3\Omega_1}{N_2N_3}\right)^2\right]\rho_{33}=0. \tag{A9}$$

After replacing $\mathrm{Re}\{\rho_{23}\}$ with ρ_{22} and ρ_{33} in Eqs. (A8) and (A9), we can find that only $\rho_{22}=\rho_{33}=0$ makes these two equations established. Applying the results to Eq. (A6), we have $\rho_{23}=0$ as well as $\rho_{32}=0$. Furthermore, we can find $\rho_{12}=\rho_{13}=\rho_{21}=\rho_{31}=0$ from applying the above results to Eqs. (A2) and (A3). As other elements drop to zero and ρ_{11} rises up to unity, the system is definitely decayed to $|\psi_1\rangle$.

[1] P. W. Shor, Algorithms for quantum computation: Discrete logarithms and factoring, in *Proceedings of the Symposium on the Foundations of Computer Science, Los Alamitos, California* (IEEE, New York, 1994), p. 124.

[2] L. K. Grover, Quantum Mechanics Helps in Searching for a Needle in a Haystack, Phys. Rev. Lett. **79**, 325 (1997).

[3] A. S. Parkins, P. Marte, P. Zoller, and H. J. Kimble, Synthesis of Arbitrary Quantum States via Adiabatic Transfer of Zeeman Coherence, Phys. Rev. Lett. **71**, 3095 (1993).

[4] R. Unanyan, M. Fleischhauer, B. W. Shore, and K. Bergmann, Robust creation and phase-sensitive probing of superposition states via stimulated Raman adiabatic passage (STIRAP) with degenerate dark states, Opt. Commun. **155**, 144 (1998).

[5] C. K. Law and J. H. Eberly, Synthesis of arbitrary superposition of Zeeman states in an atom, Opt. Express **2**, 368 (1998).

[6] N. V. Vitanov, K-A. Suominen, and B. W. Shore, Creation of coherent atomic superpositions by fractional stimulated Raman adiabatic passage, J. Phys. B: At. Mol. Opt. Phys. **32**, 4535 (1999); Z. B. Yang, H. Z. Wu, and S. B. Zheng, Robust generation of qutrit entanglement via adiabatic passage of dark states, Chin. Phys. B **19**, 094205 (2010).

[7] R. G. Unanyan, B. W. Shore, and K. Bergmann, Preparation of an N-component maximal coherent superposition state using the stimulated Raman adiabatic passage method, Phys. Rev. A **63**, 043401 (2001).

[8] Z. Kis, A. Karpati, B. W. Shore, and N. V. Vitanov, Stimulated Raman adiabatic passage among degenerate-level manifolds, Phys. Rev. A **70**, 053405 (2004).

[9] Z. Kis, N. V. Vitanov, A. Karpati, C. Barthel, and K. Bergmann, Creation of arbitrary coherent superposition states by stimulated Raman adiabatic passage, Phys. Rev. A **72**, 033403 (2005).

[10] G. Bevilacqua, G. Schaller, T. Brandes, and F. Renzoni, Implementation of stimulated Raman adiabatic passage in degenerate systems by dimensionality reduction, Phys. Rev. A **88**, 013404 (2013).

[11] G. P. Djotyan, J. S. Bakos, G. Demeter, Z. Sörlei, J. Szigeti, and D. Dzsotjan, Creation of a coherent superposition of quantum states by a single frequency-chirped short laser pulse, J. Opt. Soc. Am. B **25**, 166 (2008).

[12] L. Deng, Y. P. Niu, Y. Xiang, S. Q. Jin, and S. Q. Gong, Creation of an arbitrary coherent superposition state with chirped delayed pulses, J. Phys. B: At. Mol. Opt. Phys. **43**, 035401 (2010).

[13] N. Sandor, G. Demeter, D. Dzsotjan, and G. P. Djotyan, Coherence creation in an optically thick medium by matched propagation of a chirped-laser-pulse pair, Phys. Rev. A **89**, 033823 (2014).

[14] F. O. Prado, E. I. Duzzioni, M. H. Y. Moussa, N. G. de Almeida, and C. J. Villas-Bôas, Nonadiabatic Coherent Evolution of Two-Level Systems under Spontaneous Decay, Phys. Rev. Lett. **102**, 073008 (2009).

[15] M. J. Kastoryano, F. Reiter, and A. S. Sørensen, Dissipative Preparation of Entanglement in Optical Cavities, Phys. Rev. Lett. **106**, 090502 (2011).

[16] F. Reiter and A. S. Sørensen, Effective operator formalism for open quantum systems, Phys. Rev. A **85**, 032111 (2012).

[17] L. T. Shen, X. Y. Chen, Z. B. Yang, H. Z. Wu, and S. B. Zheng, Steady-state entanglement for distant atoms by dissipation in coupled cavities, Phys. Rev. A **84**, 064302 (2011).

[18] L. T. Shen, X. Y. Chen, Z. B. Yang, H. Z. Wu, and S. B. Zheng, Distributed entanglement induced by dissipative bosonic media, Europhys. Lett. **99**, 20003 (2012).

[19] K. W. Murch, U. Vool, D. Zhou, S. J. Weber, S. M. Girvin, and I. Siddiqi, Cavity-Assisted Quantum Bath Engineering, Phys. Rev. Lett. **109**, 183602 (2012).

[20] X. P. Zhang, L. T. Shen, Z. Q. Yin, H. Z. Wu, and Z. B. Yang, Resonator-assisted quantum bath engineering of a flux qubit, Phys. Rev. A **91**, 013825 (2015).

[21] K. Geerlings, Z. Leghtas, I. M. Pop, S. Shankar, L. Frunzio, R. J. Schoelkopf, M. Mirrahimi, and M. H. Devoret, Demonstrating a Driven Reset Protocol for a Superconducting Qubit, Phys. Rev. Lett. **110**, 120501 (2013).

[22] Y. H. Chen, Y. Xia, Q. Q. Chen, and J. Song, Fast and noise-resistant implementation of quantum phase gates and creation of quantum entangled states, Phys. Rev. A **91**, 012325 (2015).

[23] Y. Liang, S. L. Su, Q. C. Wu, X. Ji, and S. Zhang, Adiabatic passage for three-dimensional entanglement generation through quantum Zeno dynamics, Opt. Express **23**, 5064 (2015).

[24] $\Omega_p = \frac{1}{\sqrt{2}}\Omega_0 e^{-(t-\tau)^2/T^2}$ and $\Omega_s = \Omega_0[e^{-(t-\tau+28)^2/T^2} + \frac{1}{\sqrt{2}}e^{-(t-\tau)^2/T^2}]$. Ω_0 is set to be 1 unit, which is the same as Ω_1 and Ω_2 in our method. And we assume $\Omega_0 T = 20$ and $\Omega_0 \tau = 80$.

[25] B. E. Anderson, H. Sosa-Martinez, C. A. Riofrío, I. H. Deutsch, and P. S. Jessen, Accurate and Robust Unitary Transformations of a High-Dimensional Quantum System, Phys. Rev. Lett. **114**, 240401 (2015).